AD-A087 421 ILLINOIS UNIV AT URBANA-CHAMPAIGN ELECTRO-PHYSICS LAB F/G 20/5
SHORT INTENSE SUBMILLIMETER PULSE GENERATION.(U)
JUL 80 T A DETEMPLE DAAG29-79-C-0075
UNCLASSIFIED UILU-ENG-80-2546 ARO-16751/2-P NL

1 of 1
AD A
087421

END
DATE FILMED
9-80
DTIC

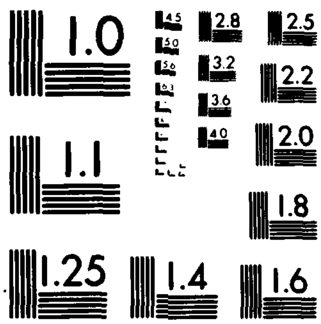

MICROCOPY RESOLUTION TEST CHART

ARO 16751.2-P

LEVEL II (12)

UILU-ENG-80-2546

ADA087421

SHORT INTENSE SUBMILLIMETER PULSE GENERATION

Final Report for the Period

July 1, 1979 to June 30, 1980

Prepared for
U. S. Army Research Office
P. O. Box 12211
Research Triangle Park, NC 27709

Contract Number
DAAG-29-C-0075

Prepared by
T. A. DeTemple
Electro-Physics Laboratory
Department of Electrical Engineering
University of Illinois
Urbana, Illinois 61801

Approved for public release; distribution unlimited.

July 1980

(9) Final, 1 Jul 79 - 30 Jun 80

Unclassified

SECURITY CLASSIFICATION OF THIS PAGE (When Data Entered)

REPORT DOCUMENTATION PAGE		READ INSTRUCTIONS BEFORE COMPLETING FORM
1. REPORT NUMBER	2. GOVT ACCESSION NO. AD-A087 421	3. RECIPIENT'S CATALOG NUMBER
4. TITLE (and Subtitle) (6) Short Intense Submillimeter Pulse Generation		5. TYPE OF REPORT & PERIOD COVERED Final 7-1-79/6-30-80
		6. PERFORMING ORG. REPORT NUMBER (14) UILU-ENG-80-2546
7. AUTHOR(s) (10) Thomas A. DeTemple	(12) 27	8. CONTRACT OR GRANT NUMBER(s) DAAG-29-79-C-0075
9. PERFORMING ORGANIZATION NAME AND ADDRESS Department of Electrical Engineering University of Illinois Urbana, IL 61801		10. PROGRAM ELEMENT, PROJECT, TASK AREA & WORK UNIT NUMBERS P-16751-P
11. CONTROLLING OFFICE NAME AND ADDRESS U.S. Army Research Office P.O. Box 12211 Research Triangle Park, NC 27709		12. REPORT DATE (11) Jul[redacted]80
		13. NUMBER OF PAGES 24
14. MONITORING AGENCY NAME & ADDRESS (if different from Controlling Office) (18) ARO (19) 16751.2-P		15. SECURITY CLASS. (of this report) Unclassified
		15a. DECLASSIFICATION/DOWNGRADING SCHEDULE

16. DISTRIBUTION STATEMENT (of this Report)

Approved for public release; distribution unlimited.

(15) DAAG29-79-C-0075

17. DISTRIBUTION ~~STATEMENT (of the abstract entered in Block 20, if different from Report)~~

18. SUPPLEMENTARY NOTES

The views, opinions, and/or findings contained in this report are those of the author(s) and should not be construed as an official Department of the Army position, policy, or decision, unless so designated by other documentation.

19. KEY WORDS (Continue on reverse side if necessary and identify by block number)

Near millimeter wave sources
Optical pumping
Mode-locking
Short pulses
Transient effects

20. ABSTRACT (Continue on reverse side if necessary and identify by block number)

The use of a mode-locked CO_2 laser for an optically pumped near millimeter wave source has been refined and extended to the generation of pulses from $C^{13}H_3F$ at 1.22mm. More refined theoretical estimates illustrate the transient nature of the conversion process in both space and time and set approximate limits on the ultimate pulse duration to be about one-half that → next page

DD FORM 1473 1 JAN 73

Unclassified

SECURITY CLASSIFICATION OF THIS PAGE (When Data Entered)

403714

of the pump. The implications are that one is not limited by the intrinsic linewidth in producing short pulse and that significant conversion may occur in modest distances, of order meters, suggesting quasi-compact sources for further experiments.

UILU-ENG-80-2546

SHORT INTENSE SUBMILLIMETER PULSE GENERATION

Final Report for the Period

July 1, 1979 to June 30, 1980

Prepared for
U. S. Army Research Office
P. O. Box 12211
Research Triangle Park, NC 27709

Contract Number
DAAG-29-C-0075

Prepared by
T. A. DeTemple
Electro-Physics Laboratory
Department of Electrical Engineering
University of Illinois
Urbana, Illinois 61801

July 1980

TABLE OF CONTENTS

I. Introduction

This final report summarizes the research conducted under the Contract DAAG 29-79-C-0075 during the period July 1, 1979 to June 30, 1980. It was the goal of this research to investigate short, intense submillimeter pulse generation obtained by mode locked optical pumping. Efforts were made towards demonstrating short pulse generation at 1.2mm and towards the general characterization of such an approach in experiment and in theory; the latter two of which will be outlined in the following two sections. The last section is devoted to the summary of this report.

II. Experiment

The technique that has been explored in this research was in the use of mode-locked optical pumping of low pressure gases, which has been previously demonstrated successfully for subnanosecond pulse generation at 385 μm in D_2O and 496 μm in $C^{12}H_3F$.[1] Recently, this approach has been extended to other transitions, e.g., 66 μm in D_2O, 193 μm in $C^{12}H_3F$ and 151 μm in NH_3.[2] This study was aimed at not only the generation of short intense pulses at 1.2mm in $C^{13}H_3F$ but also the mathematical characterization of such an optical pumping approach.

The experiment was performed in a simple single-pass configuration as is shown in Figure 1. Here the hybrid TEA-CO_2 laser, which was used for other experiments,[3,4] was

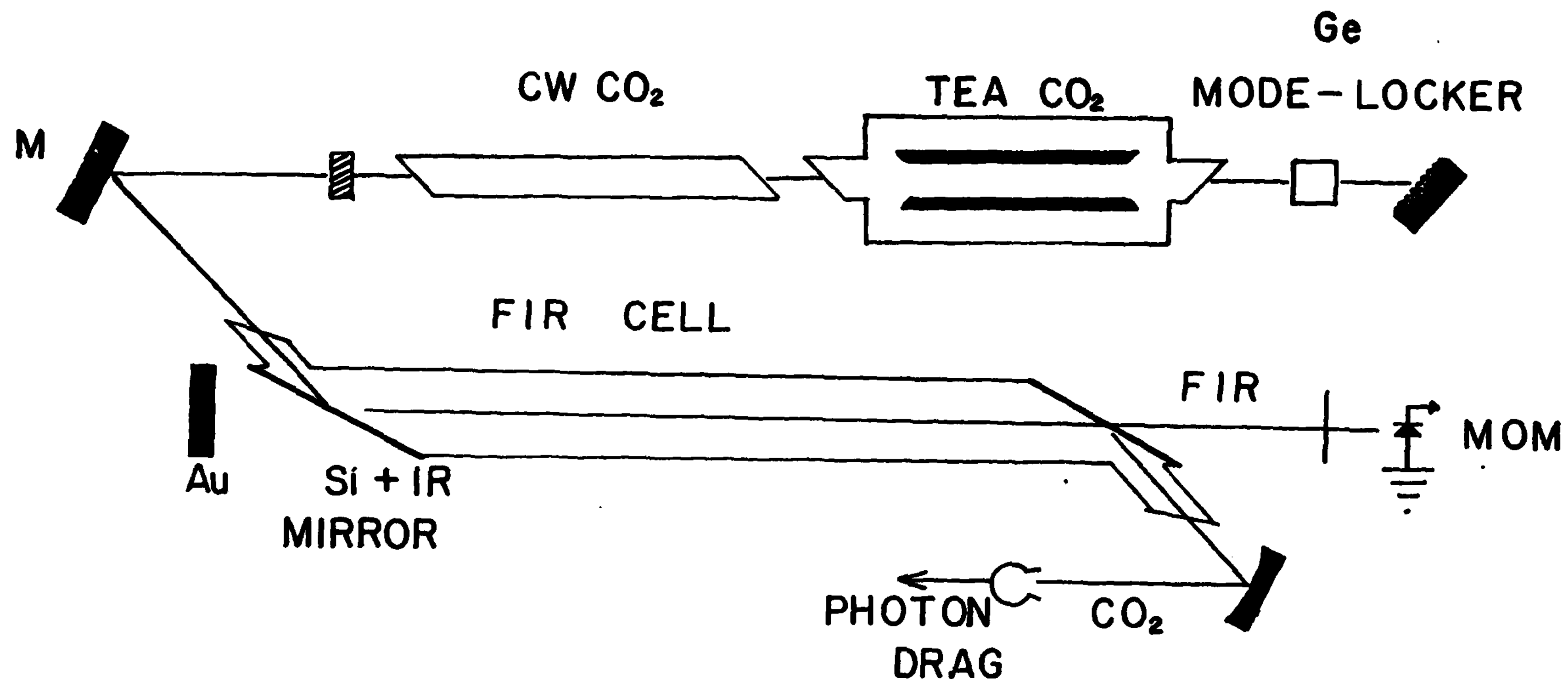

Figure 1. The experimental apparatus.

converted to a mode-locked laser with the insertion of a Ge acousto-optic modulator. This laser provided a very stable train of mode-locked pumping pulses, whose pulsewidth was variable from 2 nsec to 5 nsec, depending on the RF power applied to the modulator.[5] The Pyrex FIR waveguide was terminated with Si-Brewster window-couplers at both ends. The path of the CO_2 laser beam was such that it entered the FIR cell via the input coupler, propagated to the end and finally exited through the output coupler. Of the two possible propagation components of the FIR wave, the backward wave was fed back to the cell by a reflector at the entrance end to enhance the signal when the FIR output was not appreciable, but otherwise it was absorbed by an absorber. The CO_2 laser exiting the cell was focused onto a Ge photon drag detector to monitor the pumping pulses. The FIR pulses were detected by a tungsten wire-on-nickel MOM diode, and observed with a Tektronix 485 oscilloscope (350 MHz bandwidth).

The C^{13} isotope of methyl fluoride has a few lasing transitions at millimeter wavelengths (1.222mm, 1.207mm, 1.006mm and 0.862mm)[6] and at submillimeter wavelengths (388 μm, 412 μm) due to the hot-band transition.[7] Figure 2 shows the partial energy level diagram and some of the relevant lasing transitions, however since the operating pressure was around one torr, the dominant transition was expected to be mainly at 1.2mm.[6]

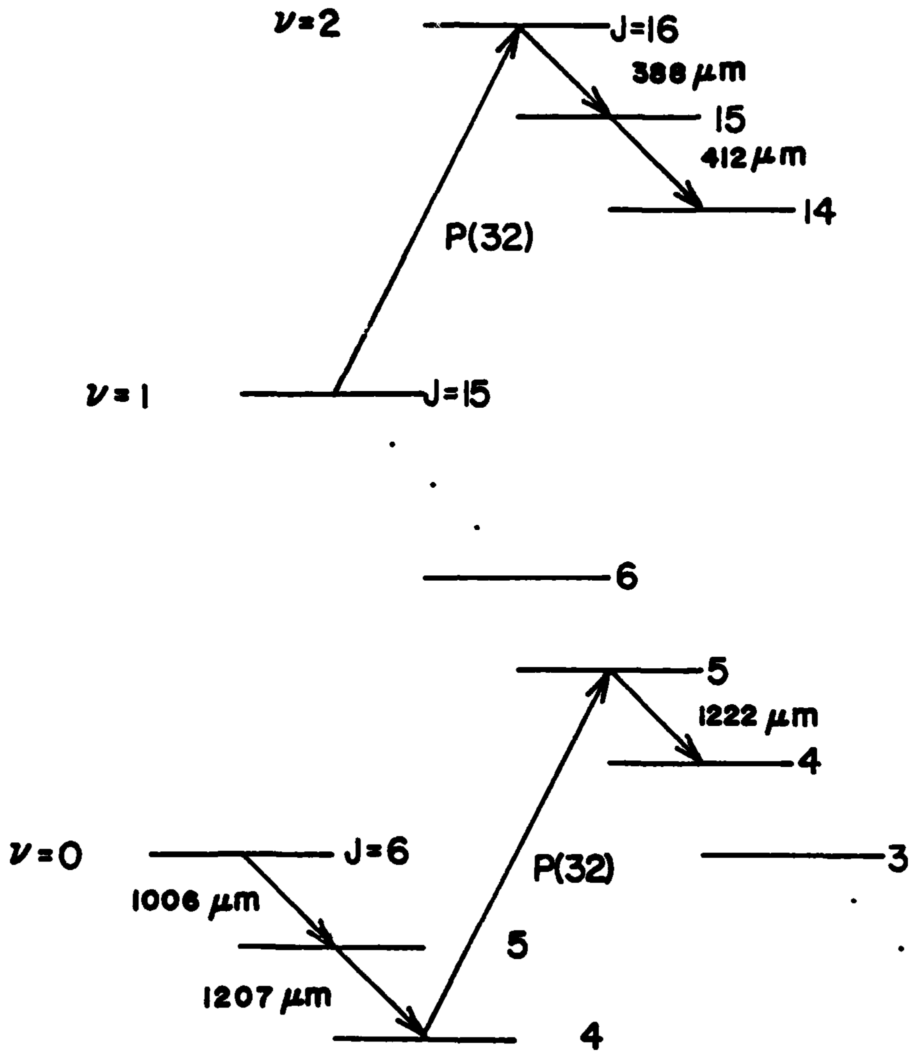

Figure 2. $C^{13}H_3F$ energy level diagram.

The pulse width observed from the mode-locked pumping scheme ranged from 5 nsec to 8 nsec, some typical pulses of which are shown in Figure 3. The pulse shape was determined to be very close to a hyperbolic secant waveform. The FIR pulse envelope delay with respect to that of pumping pulses was also measured at different pressures, and Figure 4 shows the combined signals due to the pump and the FIR pulses.

This result is compared with the data obtained from the swept-gain superradiance experiment, which is shown in Figure 5. It is noticed that there is a good agreement between the two experiments suggesting a superradiant like behavior in one case. The pulsewidth variation with the cell pressure was not significant enough to be resolvable by the present detection system. The scaling law of pulsewidth in terms of such parameters as cell pressure, pump intensity or energy and cell length is yet to be confirmed experimentally, but the following theoretical consideration suggests that some pulse width reduction be possible through various means. In summary, pulses at about the kW level and of duration $\sim T_2$ have been obtained at 1.22mm by this technique.

III. Theory

In addition to the experimental investigation, a theoretical study was also considered in order to understand the conversion dynamics of the mode-locked pumping of low pressure

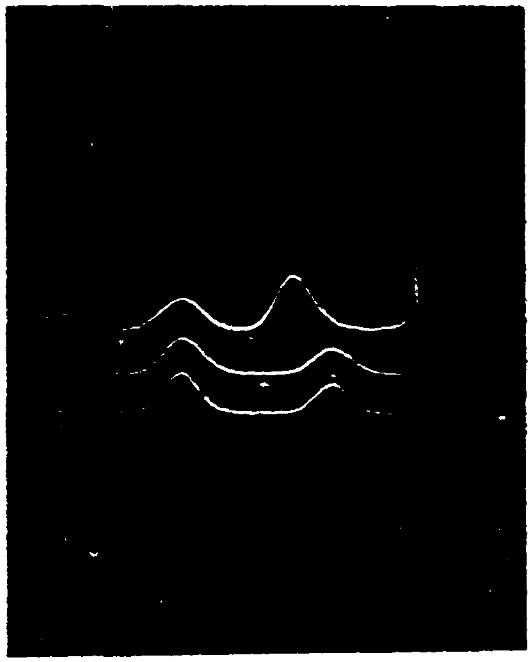

Figure 3. Typical 1.2mm pulses. This was taken at 1 torr and the cell was 3.6m long. Horizontal scale 5 nsec/div.

a)

b)

c)

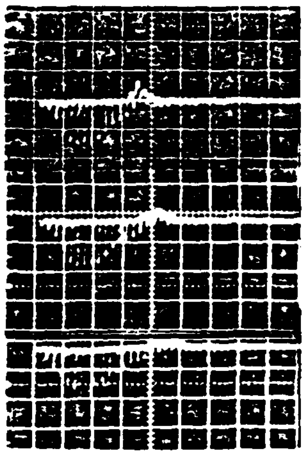

Figure 4. FIR envelope delays at three different pressures; a) 0.1 torr, b) 0.07 torr, c) 0.05 torr. The pressure was measured with a capacitive manometer. Horizontal scale, 0.1 μsec/div.

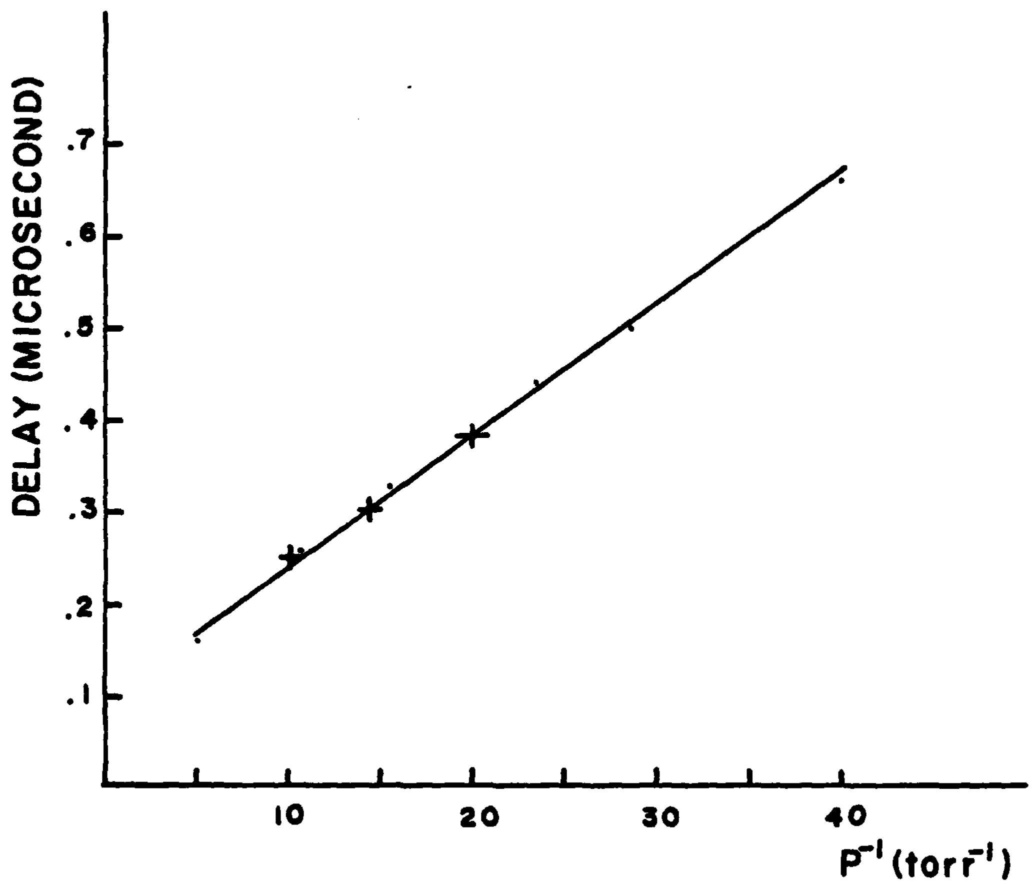

Figure 5. Comparison of delay with that of swept-gain superradiance experiment performed at Redstone. +; mode-locked pumping, •; superradiance.

gases and to assess the practicability of such an approach. In view of the fact that the pulses are shorter than the 'T_2' time scale of the medium, the conversion process belongs in the realm of a true transient phenomena. There are a few other studies that have been considered and are related to the present situation. One is the transient stimulated Raman scattering (TSRS)[8-10] and the other is the swept-gain superradiance. In this study, the near-resonance nature of the interaction precludes the former from being directly applied. The latter may be relevant at least for non-overlapping pump and FIR, but the FIR pulse evolution during the pumping period has to be included. This has been studied recently in terms of the initial tipping angle evolution during the pump pulse period.[11,12]

In this study we modelled the situation as a resonant interaction of two waves with a three-level system, and the transient analysis was comprised of solutions of the semiclassical model based on the equations of motion for the density matrix elements along with the wave equation for the FIR field. The energy level configuration for which the analysis was based is shown in Figure 6. After some standard algebraic manipulations, the following normalized set of coupled equations is obtained where t is the retarded time, $t = t - \frac{z}{v_s}$.

Diagonal Element or Population:

$$\frac{\partial N_1}{\partial t} = \frac{1}{2} E_p R_{13} - \frac{(N_1 - N_1^e)}{T_1}$$

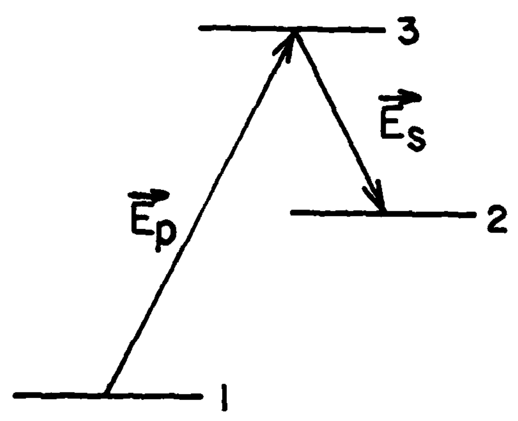

Figure 6. The energy level diagram for the analysis.

$$\frac{\partial N_2}{\partial t} = -\frac{1}{2} E_s R_{32} - \frac{N_2}{T_1}$$

$$\frac{\partial N_3}{\partial t} = -\frac{1}{2} E_p R_{13} + \frac{1}{2} E_s R_{32} - \frac{N_3}{T_1}$$

<u>Off-diagonal Element or Polarization</u>

$$\frac{\partial R_{13}}{\partial t} = -E_p(N_1-N_3) - \frac{1}{2} E_s R_{12} - \frac{R_{13}}{T_2}$$

$$\frac{\partial R_{32}}{\partial t} = -E_s(N_3-N_2) + \frac{1}{2} E_p R_{12} - \frac{R_{32}}{T_2}$$

$$\frac{\partial R_{12}}{\partial t} = -\frac{1}{2} E_p R_{32} + \frac{1}{2} E_s R_{13} - \frac{R_{12}}{T_2}$$

<u>Field Growth</u>

$$\frac{\partial E_s}{\partial z} = -g\, R_{32} - \kappa E_s$$

In these equations, the following definitions are introduced:

Rabi frequency: $E_p = \vec{\mu}_{IR} \cdot \vec{E}_p/\hbar$, $E_s = \vec{\mu}_{PER} \cdot \vec{E}_s/\hbar$, μ_{IR} = IR transition dipole moment ($\sim$ 0.1D), μ_{PER} = FIR transition moment ($\sim$ 1D), N_1^e = equilibrium population in the ground state, $g = k_s \mu_{PER}^2/4\hbar\varepsilon_o$ and κ = linear field loss coefficient representing, for example, diffraction losses. In this simplified treatment, pump depletion is neglected.

We were interested in the solutions of these equations in two different limits. One was the time response of the system to the repetitive pumping by the periodic pulses, and the other was the FIR pulse evolution both in time and space in a single pulse scheme. First, a numerical integration was performed on these equations for a train of mode-locked pumping pulses with a parabolic power spectrum. Here, the M-degeneracy factor was included in the analysis and the FIR field was assumed to have reached the so-called 'steady-state', i.e., space independent. This limit was described in more detail in an early report[13] so only some of the salient features will be discussed here.

Figure 7 depicts typical pump and FIR pulses (from the numerical selection) in the initial portion of the train sharing the process of FIR pulse stabilization. Once the FIR has been stabilized, the periodic regeneration is maintained. In Figure 8, the effect of the peak pump intensity variation on the FIR pulse shape is shown. For a weak pump, the FIR pulse shape is closely given by a hyperbolic secant waveform. As the pump intensity is increased, the delay between the two peaks decreases as does the FIR pulsewidth, and for even a stronger pump the FIR pulse leads the pump pulse. The latter has been observed in the other experiments.[2] The main point to note from these is that pulse widths of about half the pump pulse width are predicted.

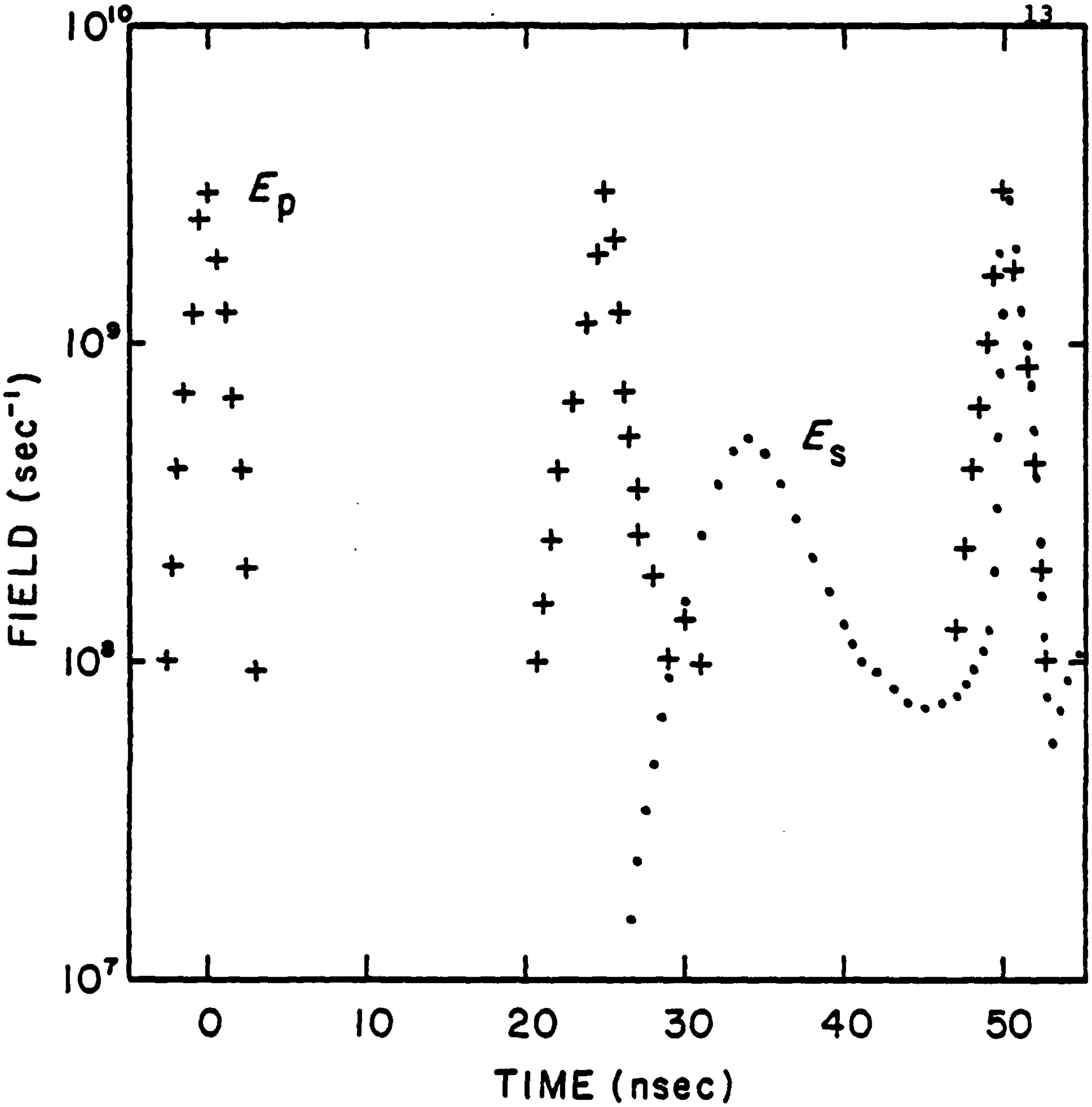

Figure 7. Normalized fields (Rabi frequencies) versus time. The calculation was started at t=-3 nsec with an initial condition of $E_s(o)=1$. For t > 50 nsec, the system has stabilized.[5] The pump field is approximately 1 MW/cm^2, 1.2 nsec duration.

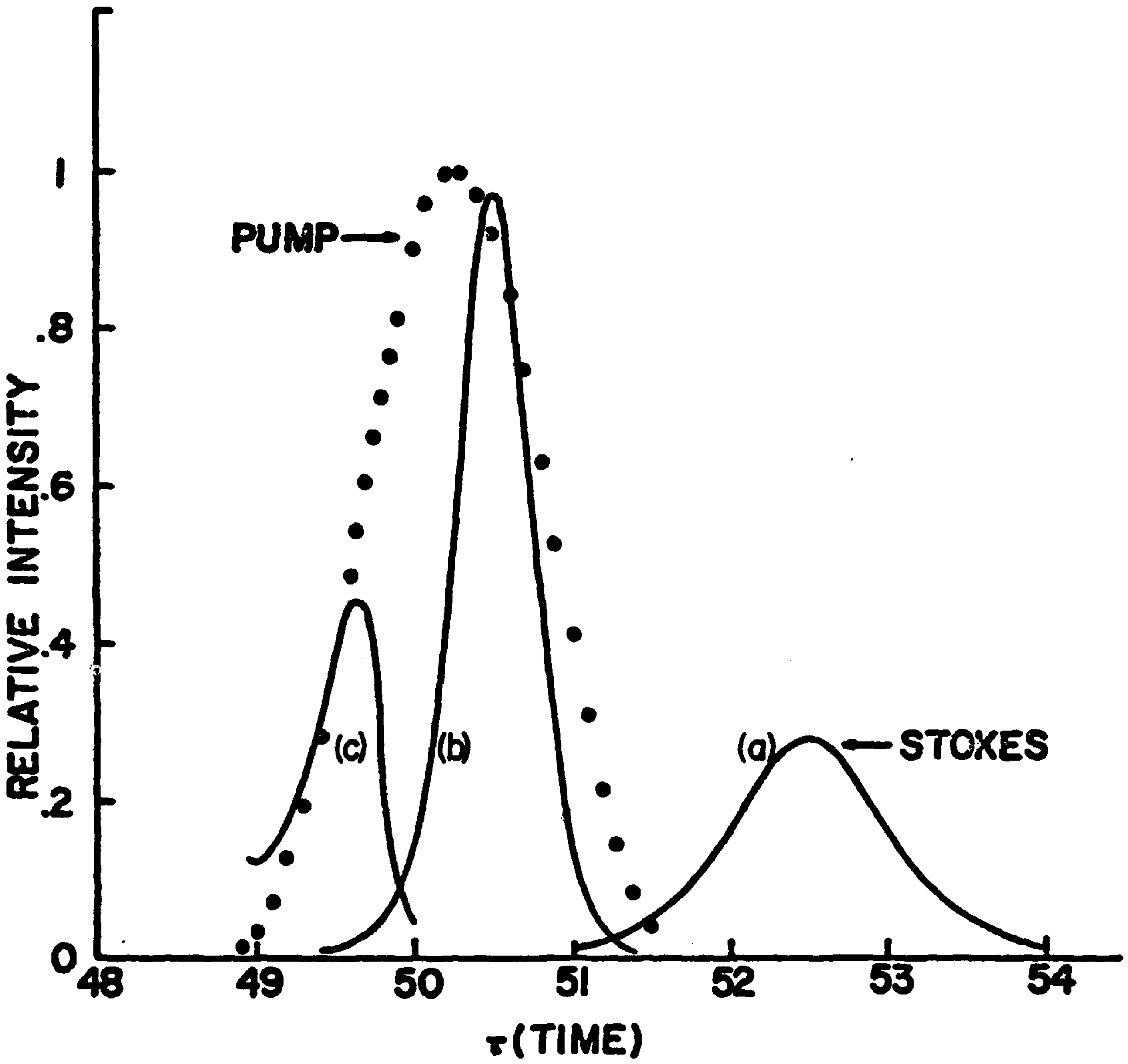

Figure 8. Comparison of the Stokes pulses at different pump intensities. The peak pump intensity for each case is, a) 10^5 W/cm^2, b) 10^6 W/cm^2, and c) 10^7 W/cm^2.

In a second inquiry, the analytical solution of the equations was pursued. Here the Stark shift term due to the FIR field was neglected and the solution was obtained for the FIR pulse where the pump pulse width was restricted to $t_p \ll T_2$. The calculational details are presented in the Appendix. After solving the equations in a self-consistent manner, the FIR field is obtained as Equation (A-10)

$$E_s(t,z) = E_s(t,o) + \sqrt{gz}\,\sin\frac{\theta(t)}{2} \times \int_0^t \frac{E_s(t-t',o)}{\sin\frac{\theta(t-t')}{2}}\,\frac{I_1\left[2\sqrt{gz\tau(t')}\right]}{\sqrt{\tau(t')}}\,\sin^2\frac{\theta(t')}{2}\,dt'$$

where

$$\theta(t) = \int_0^t E_p(t')dt', \text{ the pump pulse area,}$$

$$E_s(t,o) = \text{FIR initiating field at } z=0 \cong E_{so}$$

$$I_1 = \text{modified Bessel function of the first kind, and}$$

$$\tau(t') = \int_0^{t'} \sin^2\frac{\theta(t'')}{2}\,dt''.$$

Invoking the asymptotic limit of I_1 for a small argument, the FIR field is simplified as

$$E_s(t,z) \cong E_{so} + gzE_{so}\,\sin\frac{\theta(t)}{2}\int_0^t \frac{\sin^2\frac{\theta(t')}{2}}{\sin\frac{(t-t')}{2}}\,dt'$$

which shows a linear growth in z. For large agrument, $I_1(x) \to (2\pi x)^{-\frac{1}{2}} e^x$ so that

$$E_s(t,z) \approx E_{so} \frac{(gz)^{\frac{1}{4}}}{2\sqrt{\pi}} \sin \frac{\theta(t)}{2} \int_0^t \frac{\sin^2 \frac{\theta(t')}{2}}{\sin \frac{\theta(t-t')}{2}} \frac{e^{2\sqrt{gz\tau(t')}}}{[\tau(t)]^{3/4}} dt'$$

Since $\tau(t)$ is an integral of a squared function and is expected to be a smooth function of time, this result implies a FIR field growth scaling as

$$E_s(t,z) \propto E_{so} \exp\left[2\sqrt{gz\tau}\right]$$

From these asymtotic solutions, we can see that the FIR field growth is linear in z in the beginning but as it propagates, its growth evolves to $\exp\left[2\sqrt{gz\tau}\right]$. For a rectangular pump pulse with small area, the FIR pulse can be shown to grow as $\exp(\sqrt{Gz}t^{3/2})$ where $GT_2 = gE_p^2T_2$ and is interpreted as the steady-state Raman gain. As was pointed out in the early report, this characteristic implies the temporal contraction of Stokes pulse as it propagates. The sine factor in the solution results in structure as the FIR pulse, which is the manifestation of the nutation effect caused by the pump. This is analogous to the effect of the material saturation in the TSRS.[10]

IV. Summary

In concluding, this work extends the mode-locked optical pumping technique into the mm range with the production of $\sim$ 5 nsec pulses from $C^{13}H_3F$. The theoretical description of the conversion process was also investigated in terms of the small signal and large signal growth of the FIR field with the main result being the conversion is more closely related to swept gain superradiance than to stimulated Raman emission. With these, we can set rough bounds on the shortest possible FIR pulse widths τ_F as $1.8\ T_2\kappa_F/G_F < \tau_F \lesssim t_p/2$. The lower limit comes from assuming a delta function pump and is the steady state superradiance result while the upper limit is from the numerical solutions discussed earlier. Using values appropriate to the experiments, FIR pulses in the range of 200-400 psec may be anticipated. What remains to be determined is the spatial conversion distance, overall conversion efficiency and the pulse to pulse (in the train) stability of the FIR. The latter is of interest for possible encoding schemes.

V. Appendix

After neglecting the Stark effect terms due to the FIR field, the density matrix equations can be reduced to the following set of equations appropriate to times $t \ll T_2$:

$$\frac{\partial W_{13}}{\partial t} = E_p R_{13}$$

$$\frac{\partial W_{32}}{\partial t} = -\frac{1}{2} E_p R_{13}$$

$$\frac{\partial R_{13}}{\partial t} = -E_s W_{13} \tag{A-1}$$

$$\frac{\partial R_{32}}{\partial t} = -E_s W_{32} + \frac{1}{2} E_p R_{12}$$

$$\frac{\partial R_{12}}{\partial t} = -\frac{1}{2} E_p R_{32} + \frac{1}{2} E_s R_{13}$$

where $W_{13} = N_1 - N_3$, $W_{32} = N_3 - N_2$ are population differences. Solving these equations simultaneously, the polarization element R_{32} for the FIR field is found to be given by

$$R_{32}(t,z) = -\sin\frac{\theta(t)}{2} \int_0^t E_s(t',z) \sin\frac{\theta(t')}{2}\, dt' \tag{A-2}$$

where $\theta(t') = \int_0^{t'} E_p dt$, the pump pulse area.

Substituting this into the wave equation for the FIR field and neglecting the loss term, one obtains

$$\frac{\partial E_s(t,z)}{\partial z} = g \sin \frac{\theta(t)}{2} \int_0^t E_s(t',z) \sin \frac{\theta(t')}{2}\, dt' \tag{A-3}$$

for the field growth.

Let

$$\psi(t,z) = \int_0^t E_s(t',z) \sin \frac{\theta(t')}{2}\, dt' . \tag{A-4}$$

Then $\psi(t,z)$ satisfies the following hyperbolic equation.

$$\frac{\partial^2 \psi(t,z)}{\partial z \partial t} = g \sin^2 \frac{\theta(t)}{2}\, \psi(t,z) \tag{A-5}$$

The transformation of independent variable

$$\tau(t) = \int_0^t \sin^2 \frac{\theta(t')}{2}\, dt' \tag{A-6}$$

reduces Equation (A-5) into the standard form as

$$\frac{\partial^2 \psi(\tau,z)}{\partial z \partial \tau} = g\psi(\tau,z) \tag{A-7}$$

The boundary conditions are such that

$$\begin{aligned} \left.\frac{\partial \psi(\tau,z)}{\partial z}\right|_{\tau=0} &= 0 \\ \psi(\tau,z)\Big|_{z=0} &= \int_0^t E_s(t',o) \sin \frac{\theta(t')}{2}\, dt' \end{aligned} \tag{A-8}$$

Equation (A-7) can be solved by the Riemann's method;[14,15] the Riemann function of which is found to be

$$R(\xi,\eta;\tau,z) = I_0\left[2\sqrt{g(\tau-\xi)(z-\eta)}\right]$$

where I_0 is the modified Bessel function of zeroth order.

Therefore, the solution to Equation (A-7) can be obtained as

$$\psi(\tau,z) = \Psi(\tau,o) + \int_0^t \psi(\tau-x,o)\,\frac{\partial I_0\left[2\sqrt{gxz}\right]}{\partial x}\,dx \qquad \text{(A-9)}$$

Taking the derivatives of both sides, from Equation (A-4) the FIR field is found to be generated by

$$E_s(t,z) = E_s(t,o) + \sqrt{gz}\,\sin\frac{\theta(t)}{2}\int_0^t \frac{E_s(t-t',o)}{\sin\frac{\theta(t-t')}{2}}\,\frac{I_1\left[2\sqrt{gz\tau(t')}\right]}{\sqrt{\tau(t')}}\,dt'$$

(A-10)

which can be integrated numerically for non-simple pump pulse areas.

References

1. S. H. Lee, S. J. Petuchowski, A. T. Rosenberger, and T. A. DeTemple, Optics Lett. 4, 6 (1979).

2. W. Lemley, A. V. Nurmikko, and B. J. Clifton, Int. J. of Infrared and Millimeter Waves, 1, 85 (1980).

3. A. T. Rosenberger, S. J. Petuchowski and T. A. DeTemple, in Cooperative Effects in Matter and Radiation, C. M. Bowden, D. W. Howgate, and H. R. Robl, eds. (Plenum, NY, 1977), p. 15.

4. S. J. Petuchowski, A. T. Rosenberger, and T. A. DeTemple, IEEE J. Quan. Elec., QE-13, 475 (1977).

5. P. Bernard and P. A. Belanger, Optics Lett. 4, 196 (1979).

6. M. P. Hacker, Z. Drozdowicz, D. R. Cohn, K. Isobe and R. J. Temkin, Phys. Lett. 57A, 328 (1976).

7. W. A. Peebles, D. L. Brower, N. C. Luhman, Jr., and E. J. Danielewicz, IEEE J. Quan. Elec., QE-16, 505 (1980).

8. R. L. Carman, F. Shinizer, C. S. Wang, and N. Bloembergen, Phys. Rev. A2, 60 (1970).

9. S. A. Akhmanov, K. N. Drabovich, A. P. Sikhorukov, and A. S. Chirkin, Soviet Physics JETP, 32, 266 (1971).

10. J. N. Elgin and T. B. O'Hare, J. Phys. B12, 159 (1979).

11. C. M. Bowden and C. C. Sung, Phys. Rev. A18, 1558 (1978).

12. C. M. Bowden and C. C. Sung, Phys. Rev. A20, 2033 (1979).

13. T. A. DeTemple, UILU-ENG-79-2551 (1979), Final report for DAAG-29-77-C-0025.

14. R. Courant and D. Hilbert, Methods of Mathematical Phyics, Volume II, (Interscience, NY 1962), p. 449.

15. C. S. Wang, Phys. Rev. 182, 482 (1969).

Scientific Personnel Associated with Grant

Thomas A. DeTemple	Principle Investigator
H. Chung	Research Assistant

Thesis, Publications and Talks Associated with Grant

1. T. A. DeTemple, H. K. Chung, and S. J. Petuchowski, "Three Photon Contribution in Optically Pumped Lasers", Int. J. of Infrared and Millimeter Waves, 1, 27 (1980).

2. T. A. DeTemple, S. J. Petuchowski and H. K. Chung, "Semiclassical Treatment of Multiphoton Interactions in AC Stark Shifts", in review.

3. H. K. Chung and T. A. DeTemple, "Semiclassical Treatment of Multiphoton Interactions: Signal Flow Graph Approach", in review.

4. H. K. Chung, S. H. Lee and T. A. DeTemple, "Mode-Locked FIR Pulse Generation", Paper S-1-2, Presented at the Fourth Infrared and Submillimeter Wave Conference, Miami, 1979.

5. T. A. DeTemple, H. K. Chung and S. J. Petuchowski, "Three-Photon Contributions in Optically Pumped Lasers", Invited Paper Th-2-1, Presented at the Fourth Infrared and Submillimeter Wave Conference, Miami, 1979.